

A MULTI-HARMONIC METHOD FOR NON-LINEAR VIBRATION ANALYSIS

ALBERTO CARDONA*

INTEC (CONICET/UNL), Güemes, 3450, 3000 Santa Fe, Argentina

THIERRY COUNE† ALBERT LERUSSE† AND MICHEL GERADIN‡

LTAS, University of Liège, Rue E. Solvay, 21, B-4000 Liège, Belgium

SUMMARY

A multiharmonic method for analysis of non-linear dynamic systems submitted to periodic loading conditions is presented. The approach is based on a systematic use of the fast Fourier transform. The exact linearization of the resulting equations in the frequency domain allows to obtain full quadratic convergence rate.

1. INTRODUCTION

The analysis of the dynamic behaviour of non-linear mechanical systems—including the modelling of friction, impacts, large displacements and rotations—and submitted to periodic excitations is of great importance in engineering analysis. Examples of application can be found in machine dynamics, rotor dynamics, vehicle dynamics, helicopter rotor blade analysis, satellite dynamics, etc.

The dynamic analysis of flexible mechanisms is usually performed using direct time integration techniques.^{1,2} The approach is very efficient to analyse their transient response. However, it can lead to a lengthy calculation process in cases where the interest is focused only on the stationary behaviour under periodic loading, after all transients have been damped out from the response.

One way of computing the periodic response of a non-linear system is that of discretizing the time domain using either finite elements or finite differences, and solving the resulting non-linear algebraic with periodic boundary conditions.^{3,4}

We can mention basically two different approaches for the computation of the periodic response of a highly non-linear system, without having to solve a non-linear algebraic problem for the whole set of values along the time period. The first one is based on determining the monodromy matrix using a shooting method (see References 3–5). The second approach, which we have followed in this paper, consists in a Fourier series expansion analysis (see References 6–15).

The method of harmonic balance is well-known from the literature. Lau and Cheung,⁶ Lau *et al.*⁷ and Lau and Zang⁸ developed an incremental form of the method to improve convergence

* Professor

† Research Engineer

‡ Professor

of the non-linear algebraic problem. This proposal was followed by Pierre *et al.*,⁹ Pierre and Dowell¹⁰ to solve non-linear mechanical vibrations involving dry friction phenomenon.

Ling and Wu¹¹ proposed to use the *Fast Fourier Transform* (FFT) algorithm combined to the harmonic balance method to reduce the number of algebraic operations and minimize CPU time. The same approach was followed by other authors (References 12, 13). However, References 11 and 13 differ from each other in the way they computed the coefficients matrix for the algebraic non-linear problem. Ling and Wu¹¹ mentioned that it is possible to compute the Jacobian using the FFT, but did not give any explicit expression. They said also that in order to decrease CPU time, they avoided the computation of the Jacobian and used a Broyden method. Cameron and Griffin¹² proposed two approaches to solve the non-linear problem: a first one using a Picard iteration with a constant Jacobian and a non-linear forces vector, and a second one in which the Jacobian was evaluated by finite differences. Kim and Noah¹³ analysed the vibrations of oscillators with piecewise linear elastic force, and gave explicit expressions of the Jacobian in terms of *sine* and *cosine* functions for this case.

In order to make the method computationally efficient, we also make use of the FFT algorithm in a systematic way. After projecting the system of non-linear equilibrium equations into the frequency domain, we get a non-linear system of algebraic equations in which the unknowns are the Fourier coefficients of the FFT of the displacements. This system is solved using a Newton–Raphson method. Differently from what other authors have made, we compute explicitly the terms of the coefficients matrix of this new non-linear system as the linear combination of some terms of the Fourier transform of the tangent matrices computed in the time domain. In this way, since we get an exact linearization, we obtain a full quadratic convergence rate.

Two examples of application are shown. The first one is a spring/mass/double-stop system illustrating the capabilities of the method to handle impact situations. The second example is a clamped beam with a dry-friction damper for which numerical results are compared with those obtained in an experimental set-up.¹⁶

2. FORMULATION OF PERIODIC NON-LINEAR DYNAMICS PROBLEMS

We are interested in computing the solution $\mathbf{x}(t)$ to a non-linear dynamic problem with periodic loading

$$\mathbf{m}\ddot{\mathbf{x}} + \mathbf{g}(\mathbf{x}, \dot{\mathbf{x}}) = \mathbf{f}(t), \quad \mathbf{f}(t + T_f) = \mathbf{f}(t) \quad (1)$$

where \mathbf{m} is the mass matrix, \mathbf{g} is the non-linear internal forces vector which depends on displacements and velocities and \mathbf{f} is the periodic forcing vector with period T_f .

We sample the solution \mathbf{x} at N time instants:

$$\mathbf{x}(k \Delta t) = \mathbf{x}_k, \quad k = 0, 1, \dots, N - 1 \quad (2)$$

We also make the hypothesis that the solution \mathbf{x} is periodic. Then, we can express \mathbf{x} as a real Fourier expansion in terms of N components $\mathbf{X}_{n,m}$:

$$\mathbf{x}_k = \frac{1}{\sqrt{2N}} \left(\mathbf{X}_{0,0} + 2 \sum_{n=1}^{N/2-1} (C_{kn,0} \mathbf{X}_{n,0} + C_{kn,1} \mathbf{X}_{n,1}) + (-1)^k \mathbf{X}_{N/2,0} \right) \quad (3)$$

$\mathbf{X}_{n,m}$ corresponds to the n th term of the Fourier expansion with phase m (m can be equal to 0 or 1) and coefficients $C_{kn,m}$ are, by definition,

$$C_{kn,m} = \cos\left(\frac{2\pi kn}{N} - m\frac{\pi}{2}\right) = \cos\left(\frac{2\pi n}{T} k \frac{T}{N} - m\frac{\pi}{2}\right) = \cos\left(\frac{2\pi n}{T} t_k - m\frac{\pi}{2}\right)$$

Here T is the period of analysis, which in a general case can be different from the period of excitation. When looking for subharmonic response, we make $T = kT_f$ where k is an integer defining the subharmonics order.

Equation (3) is, in fact, the inverse Fourier transform of $\mathbf{X}_{n,m}$. We will note it syntactically in the form

$$\mathbf{x}_k = \text{ift}_k^{n,m}(\mathbf{X}_{n,m}) \tag{4}$$

The number of harmonics necessary for convergence is usually much smaller than the total number of harmonics present in the model. We can further assume that only some lower harmonics contribute to the response and reduce the Fourier expansion

$$\mathbf{x}_k = \frac{1}{\sqrt{2N}} \left(\mathbf{X}_{0,0} + 2 \sum_{n=1}^{NH} \sum_{m=0}^1 C_{kn,m} \mathbf{X}_{n,m} \right) \tag{5}$$

with $NH \ll N/2 - 1$ being the number of harmonics retained in the expansion.

Velocities and accelerations are computed by time differentiation of equation (3):

$$\begin{aligned} \dot{\mathbf{x}}_k &= 2 \frac{1}{\sqrt{2N}} \frac{2\pi}{T} \sum_{n=1}^{N/2-1} n (-C_{kn,1} \mathbf{X}_{n,0} + C_{kn,0} \mathbf{X}_{n,1}) \\ \ddot{\mathbf{x}}_k &= -2 \frac{1}{\sqrt{2N}} \left(\frac{2\pi}{T} \right)^2 \sum_{n=1}^{N/2-1} n^2 (C_{kn,0} \mathbf{X}_{n,0} + C_{kn,1} \mathbf{X}_{n,1}) \end{aligned} \tag{6}$$

3. FOURIER GALERKIN NON-LINEAR SOLUTION

Let us first pose the problem of finding a solution for a non-linear statics problem using a Fourier expansion. The system to be analysed reads

$$\mathbf{r}(k) = \mathbf{r}_k = \mathbf{0}, \quad k = 0, 1, \dots, N - 1 \tag{7}$$

Parameter k has the meaning of the dimension along which we want the Fourier expansion to be performed (i.e. time, angle, length, etc.).

Instead of verifying the strong form of equilibrium (7), we will ask to verify the following weak form:

$$\mathbf{R}_{l,m} = \begin{cases} \frac{1}{2} \sqrt{\frac{2}{N}} \sum_{k=0}^{N-1} C_{kl,0} \mathbf{r}_k = \mathbf{0}, & l = 0, N/2, m = 0 \\ \sqrt{\frac{2}{N}} \sum_{k=0}^{N-1} C_{kl,m} \mathbf{r}_k = \mathbf{0}, & l = 1, 2, \dots, N/2 - 1, m = 0, 1 \end{cases} \tag{8}$$

Note that there are only N values of $\mathbf{R}_{l,m}$ since it is trivial to verify that

$$\mathbf{R}_{0,1} = \mathbf{R}_{N/2,1} = \mathbf{0}$$

This equation is almost coincident with the direct Fourier transform of \mathbf{r}_k . Terms $\mathbf{R}_{0,0}$ and $\mathbf{R}_{N/2,0}$ have been affected by a coefficient one-half to obtain a symmetric tangent matrix (see later). In what follows we will talk of $\mathbf{R}_{l,m}$ as of the Fourier transform of \mathbf{r}_k , but keep in mind the differences.

We will represent equation (8) in the compact form

$$\mathbf{R}_{l,m} = \text{ft}_{l,m}^k(\mathbf{r}_k) = \mathbf{0} \tag{9}$$

This is a system of non-linear equations with unknowns $\mathbf{X}_{l,m}$. This problem can be illustrated by the following diagram:

$$\begin{array}{ccc} \mathbf{x}_k & \text{ift}_{l,m}^k & \mathbf{X}_{l,m} \\ \mathbf{r}(\cdot) & & \mathbf{R}(\cdot) \\ \mathbf{r}_k & \text{ft}_{l,m}^k & \mathbf{R}_{l,m} \end{array}$$

which shows how to switch from frequency to temporal domain in order to compute the solution. The residual vector can be written in the form

$$\begin{aligned} \mathbf{R}_{l,m} &= \text{ft}_{l,m}^k(\mathbf{r}(\mathbf{x}_k)) \\ &= \text{ft}_{l,m}^k\left(\mathbf{r}\left(\frac{1}{\sqrt{2N}}\left(\mathbf{X}_{0,0} + 2\sum_{m=0}^1 \sum_{n=1}^{N/2-1} C_{kn,m} \mathbf{X}_{n,m} + (-1)^k \mathbf{X}_{N/2,0}\right)\right)\right) \end{aligned} \quad (10)$$

In order to solve this system of non-linear equations, we will use the method of Newton-Raphson. We will then be interested in computing the matrix of coefficients

$$\mathbf{S} = \left[\frac{\partial \mathbf{R}_{l,m}}{\partial \mathbf{X}_{n,s}} \right] \quad (11)$$

Let us note \mathbf{k}_k the tangent stiffness (derivative of the non-linear force \mathbf{r}) evaluated at \mathbf{x}_k :

$$\mathbf{k}_k = \frac{\partial \mathbf{r}}{\partial \mathbf{x}}(\mathbf{x}_k) \quad (12)$$

Let us also note $\mathbf{K}_{l,m}$ the Fourier transform of \mathbf{k}_k :

$$\mathbf{K}_{l,m} = \text{ft}_{l,m}^k(\mathbf{k}_k) \quad (13)$$

To differentiate the residual vector, we use the following trigonometric identities:

$$\begin{aligned} 2C_{kl,0} C_{kn,0} &= C_{k(l+n),0} + C_{k(l-n),0} \\ 2C_{kl,0} C_{kn,1} &= C_{k(l+n),1} + C_{k(l-n),1} \\ 2C_{kl,1} C_{kn,0} &= C_{k(l-n),1} + C_{k(l+n),1} \\ 2C_{kl,1} C_{kn,1} &= C_{k(l-n),0} + C_{k(l+n),0} \end{aligned} \quad (14)$$

Then

$$\begin{aligned} \frac{\partial \mathbf{R}_{l,0}}{\partial \mathbf{X}_{n,0}} &= \sqrt{\frac{2}{N}} \sum_{k=0}^{N-1} C_{kl,0} \mathbf{k}_k \frac{1}{\sqrt{2N}} 2C_{kn,0} \\ &= \frac{1}{\sqrt{2N}} \left(\sqrt{\frac{2}{N}} \sum_{k=0}^{N-1} C_{k(l+n),0} \mathbf{k}_k + \sqrt{\frac{2}{N}} \sum_{k=0}^{N-1} C_{k(l-n),0} \mathbf{k}_k \right) \\ &= \frac{1}{\sqrt{2N}} (\mathbf{K}_{(l+n),0} + \mathbf{K}_{(l-n),0}) \end{aligned} \quad (15)$$

A similar procedure is applied to the other components to get

$$\frac{\partial \mathbf{R}_{l,0}}{\partial \mathbf{X}_{n,1}} = \sqrt{\frac{2}{N}} \sum_{k=0}^{N-1} C_{kl,0} \mathbf{k}_k \frac{1}{\sqrt{2N}} 2C_{kn,1} = \frac{1}{\sqrt{2N}} (\mathbf{K}_{(l+n),1} + \mathbf{K}_{(l-n),1})$$

$$\frac{\partial \mathbf{R}_{l,1}}{\partial \mathbf{X}_{n,0}} = \sqrt{\frac{2}{N}} \sum_{k=0}^{N-1} C_{kl,0} \mathbf{k}_k \frac{1}{\sqrt{2N}} 2C_{kn,0} = \frac{1}{\sqrt{2N}} (\mathbf{K}_{(l-n),1} + \mathbf{K}_{(l+n),1}) \tag{16}$$

$$\frac{\partial \mathbf{R}_{l,1}}{\partial \mathbf{X}_{n,1}} = \sqrt{\frac{2}{N}} \sum_{k=0}^{N-1} C_{kl,1} \mathbf{k}_k \frac{1}{\sqrt{2N}} 2C_{kn,1} = \frac{1}{\sqrt{2N}} (\mathbf{K}_{(l-n),0} + \mathbf{K}_{(l+n),0})$$

Finally, the tangent matrix for our non-linear problem is

$$\left[\frac{\partial \mathbf{R}_{l,m}}{\partial \mathbf{X}_{n,s}} \right] = \frac{1}{\sqrt{2N}} \begin{bmatrix} \frac{1}{2} \mathbf{K}_{0,0} & \cdots & \mathbf{K}_{n,0} & \mathbf{K}_{n,1} & \cdots & \frac{1}{2} \mathbf{K}_{N/2,0} \\ \vdots & & \vdots & \vdots & & \vdots \\ \mathbf{K}_{l,0} & & \mathbf{K}_{l+n,0} + \mathbf{K}_{l-n,0} & \mathbf{K}_{l+n,1} - \mathbf{K}_{l-n,1} & & \mathbf{K}_{N/2-l,0} \\ \mathbf{K}_{l,1} & & \mathbf{K}_{l-n,1} + \mathbf{K}_{l+n,1} & \mathbf{K}_{l-n,0} - \mathbf{K}_{l+n,0} & & \mathbf{K}_{N/2-l,1} \\ \vdots & & \vdots & \vdots & & \vdots \\ \frac{1}{2} \mathbf{K}_{N/2,0} & \cdots & \mathbf{K}_{N/2-n,0} & \mathbf{K}_{N/2-n,1} & \cdots & \frac{1}{2} \mathbf{K}_{0,0} \end{bmatrix} \tag{17}$$

This coefficient matrix is symmetric.

In the case \mathbf{k} is constant, the tangent matrix can be simplified to

$$\left[\frac{\partial \mathbf{R}_{l,m}}{\partial \mathbf{X}_{n,s}} \right] = \mathbf{k} \begin{bmatrix} \frac{1}{2} \mathbf{1} & \cdots & \mathbf{0} & \mathbf{0} & \cdots & \mathbf{0} \\ \vdots & & \vdots & \vdots & & \vdots \\ \mathbf{0} & & \delta_{ln} \mathbf{1} & \mathbf{0} & & \mathbf{0} \\ \mathbf{0} & & \mathbf{0} & \delta_{ln} \mathbf{1} & & \mathbf{0} \\ \vdots & & \vdots & \vdots & & \vdots \\ \mathbf{0} & \cdots & \mathbf{0} & \mathbf{0} & \cdots & \frac{1}{2} \mathbf{1} \end{bmatrix} \tag{18}$$

Similar simplified expressions can be found if \mathbf{k} is a polynomial function of the displacements, which is usually the case in geometric non-linear problems.

4. FOURIER GALERKIN DYNAMIC SOLUTION

Let us now compute the weak solution to the original non-linear dynamics problem (1) using a Fourier Galerkin method. In this case, the residual vector reads

$$\mathbf{R}_{l,m} = \begin{cases} \frac{1}{2} \sqrt{\frac{2}{N}} \sum_{k=0}^{N-1} C_{kl,0} (\mathbf{m} \ddot{\mathbf{x}}_k + \mathbf{g}(\mathbf{x}_k, \dot{\mathbf{x}}_k) - \mathbf{f}_k) = \mathbf{0}, & l = 0, N/2, m = 0 \\ \sqrt{\frac{2}{N}} \sum_{k=0}^{N-1} C_{kl,m} (\mathbf{m} \ddot{\mathbf{x}}_k + \mathbf{g}(\mathbf{x}_k, \dot{\mathbf{x}}_k) - \mathbf{f}_k) = \mathbf{0}, & l = 1, 2, \dots, N/2 - 1, m = 0, 1 \end{cases} \tag{19}$$

We will search for a periodic solution to this problem using a Newton–Raphson method. The coefficient matrix can now be seen as made up by three components:

$$\mathbf{S} = \left[\frac{\partial \mathbf{R}_{l,m}}{\partial \mathbf{X}_{n,s}} \right] = \mathbf{S}_x + \mathbf{S}_{\dot{x}} + \mathbf{S}_{\ddot{x}} \tag{20}$$

where S_x is the contribution arising from stiffness, $S_{\dot{x}}$ is the contribution from damping and $S_{\ddot{x}}$ is the mass contribution to the dynamic stiffness S . It can be easily shown that these terms are

$$S_x = \frac{1}{\sqrt{2N}} \begin{bmatrix} \frac{1}{2}K_{0,0} & \cdots & K_{n,0} & K_{n,1} & \cdots & \frac{1}{2}K_{N/2,0} \\ \vdots & & & & & \vdots \\ K_{l,0} & K_{l+n,0} + K_{l-n,0} & K_{l+n,1} - K_{l-n,1} & & & K_{N/2-l,0} \\ K_{l,1} & K_{l-n,1} + K_{l+n,1} & K_{l-n,0} - K_{l+n,0} & & & K_{N/2-l,1} \\ \vdots & & & & & \vdots \\ \frac{1}{2}K_{N/2,0} & \cdots & K_{N/2-n,0} & K_{N/2-n,1} & \cdots & \frac{1}{2}K_{0,0} \end{bmatrix} \quad (21)$$

$$S_{\dot{x}} = \frac{2\pi}{T} \frac{1}{\sqrt{2N}} \begin{bmatrix} 0 & \cdots & -nC_{n,1} & nC_{n,0} & \cdots & 0 \\ \vdots & & & & & \vdots \\ 0 & n(C_{l-n,1} - C_{l+n,1}) & n(C_{l+n,0} + C_{l-n,0}) & & & 0 \\ 0 & n(C_{l+n,0} - C_{l-n,0}) & n(C_{l-n,1} + C_{l+n,1}) & & & 0 \\ \vdots & & & & & \vdots \\ 0 & \cdots & -nC_{N/2-n,1} & nC_{N/2-n,0} & \cdots & 0 \end{bmatrix} \quad (22)$$

$$S_{\ddot{x}} = \left(\frac{2\pi}{T}\right)^2 \frac{1}{\sqrt{2N}} \begin{bmatrix} 0 & \cdots & n^2M_{n,0} & n^2M_{n,1} & \cdots & 0 \\ \vdots & & & & & \vdots \\ 0 & n^2(M_{l+n,0} + M_{l-n,0}) & n^2(M_{l+n,1} + M_{l-n,1}) & & & 0 \\ 0 & n^2(M_{l-n,1} + M_{l+n,1}) & n^2(M_{l-n,0} - M_{l+n,0}) & & & 0 \\ \vdots & & & & & \vdots \\ 0 & \cdots & -n^2M_{N/2-n,0} & n^2M_{N/2-n,1} & \cdots & 0 \end{bmatrix} \quad (23)$$

where

$$C_{l,m} = ft_{l,m}^k(\mathbf{c}_k), \quad M_{l,m} = ft_{l,m}^k(\mathbf{m}_k) \quad (24)$$

and $\mathbf{c}_k, \mathbf{m}_k$ are the tangent damping and mass matrices (derivatives of the non-linear force \mathbf{r} with respect to velocities and accelerations) evaluated at \mathbf{x}_k :

$$\mathbf{c}_k = \frac{\partial \mathbf{r}}{\partial \dot{\mathbf{x}}}(\mathbf{x}_k), \quad \mathbf{m}_k = \frac{\partial \mathbf{r}}{\partial \ddot{\mathbf{x}}}(\mathbf{x}_k) \quad (25)$$

Again, in the case \mathbf{k}, \mathbf{c} or \mathbf{m} are constants, the latter matrices can be simplified leading to an uncoupling between different harmonics:

$$S_x = \mathbf{k} \begin{bmatrix} \frac{1}{2}\mathbf{1} & \cdots & \mathbf{0} & \mathbf{0} & \cdots & \mathbf{0} \\ \vdots & & & & & \vdots \\ \mathbf{0} & & \delta_{ln}\mathbf{1} & \mathbf{0} & & \mathbf{0} \\ \mathbf{0} & & \mathbf{0} & \delta_{ln}\mathbf{1} & & \mathbf{0} \\ \vdots & & & & & \vdots \\ \mathbf{0} & \cdots & \mathbf{0} & \mathbf{0} & \cdots & \frac{1}{2}\mathbf{1} \end{bmatrix} \quad (26)$$

$$\mathbf{S}_i = \frac{2\pi}{T} \mathbf{c} \begin{bmatrix} \mathbf{0} & \dots & \mathbf{0} & \mathbf{0} & \dots & \mathbf{0} \\ \vdots & & & & & \vdots \\ \mathbf{0} & & \mathbf{0} & \delta_{in} n \mathbf{1} & & \mathbf{0} \\ \mathbf{0} & & -\delta_{in} n \mathbf{1} & \mathbf{0} & & \mathbf{0} \\ \vdots & & & & & \vdots \\ \mathbf{0} & \dots & \mathbf{0} & \mathbf{0} & \dots & \mathbf{0} \end{bmatrix} \quad (27)$$

$$\mathbf{S}_i = -\left(\frac{2\pi}{T}\right)^2 \mathbf{m} \begin{bmatrix} \mathbf{0} & \dots & \mathbf{0} & \mathbf{0} & \dots & \mathbf{0} \\ \vdots & & & & & \vdots \\ \mathbf{0} & & \delta_{in} n^2 \mathbf{1} & \mathbf{0} & & \mathbf{0} \\ \mathbf{0} & & \mathbf{0} & \delta_{in} n^2 \mathbf{1} & & \mathbf{0} \\ \vdots & & & & & \vdots \\ \mathbf{0} & \dots & \mathbf{0} & \mathbf{0} & \dots & \mathbf{0} \end{bmatrix} \quad (28)$$

Once, we have determined the coefficients matrix \mathbf{S} , we can very efficiently implement a Newton-Raphson procedure to compute the solution of the non-linear problem (19).

5. NUMERICAL APPLICATIONS

A computer program was made following the theory outlined in the previous sections, using the well-known *Matlab* software. The objective was to test the method and see the feasibility of application to analyse dynamic vibration problems coming from the mechanical industry. In particular, two examples are presented here: the first one is a problem involving contact, while the second example concerns a test set-up to analyse dry-friction phenomena for which we disposed of experimental results for comparison.

5.1. Spring/mass/double-stop system

The response of a spring/mass/double-stop system submitted to an harmonic excitation at its base is first analysed (see Figure 1).

The system consists of a spring, whose stiffness depends on elongation as indicated in Figure 1, with stiffness constants $k_1 = 1.20 \times 10^4$ N/m, $k_2 = 1.26 \times 10^7$ N/m and $l_0 = 1.5 \times 10^{-5}$ m. The spring supports a unit mass at its extreme. The system is submitted to a sinusoidal acceleration of 9.81 m/s² at its base, with frequency varying from 300 to 160 Hz.

The response was computed using a total of 128 points to represent the time series, and included 13 harmonics in the multiharmonic model. First, we got the solution for an excitation frequency of 300 Hz. Afterwards, we spanned the frequency band from 300 to 160 Hz with an increment of -5 Hz at each step.

Figure 2 displays the root mean square function of vertical absolute acceleration \ddot{x}_1 at the mass. We see that the acceleration increases smoothly when decreasing the excitation frequency up to the point of 180 Hz where the curve presents a sharp discontinuity.

Figure 3 shows the evolution in time of the displacement and velocity of the mass when the system is submitted to an excitation of 190 Hz. We see that the mass touches the lower limit at $t = 1.25 \times 10^{-3}$ and rebounds. A discontinuity in the evolution of velocity is clearly evidenced at this point.

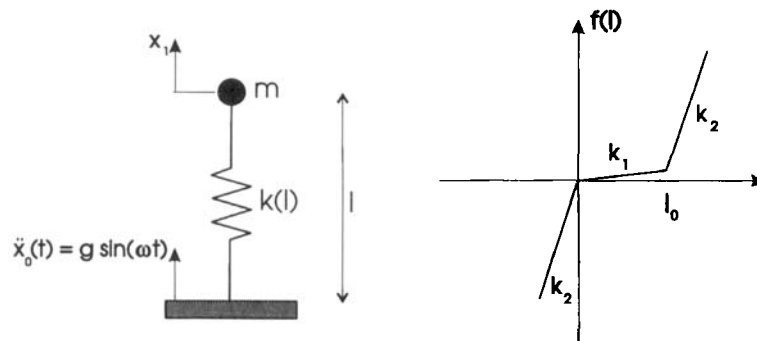
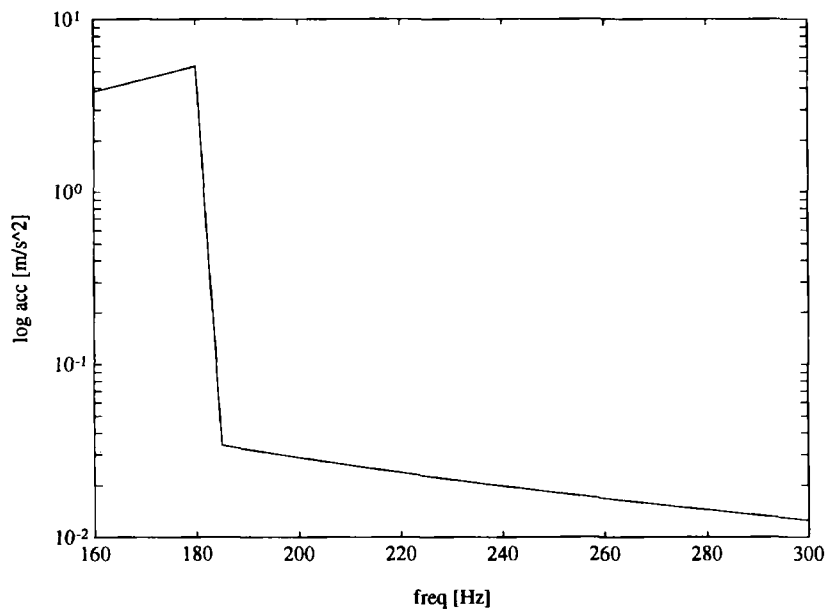


Figure 1. Spring/mass/double-stop

Figure 2. Root mean square of absolute accelerations \ddot{x}_1

In Figure 4 we compare the vertical displacement of the mass with the displacement of the base and of the upper limit of the system. We see that, in fact, the mass remains almost fixed with respect to the oscillating frame.

When the frequency of excitation decreases below 180 Hz, the amplitude of motion of the excitation frame is such that the mass comes also into contact with the upper limit. At this point the nature of motion changes completely. Figure 5 displays the displacement and velocity evolution of the mass in this case. We can appreciate that it bounces continuously between the lower and upper limits given by the excitation frame. We see also that the dominant frequency of response is twice the excitation frequency.

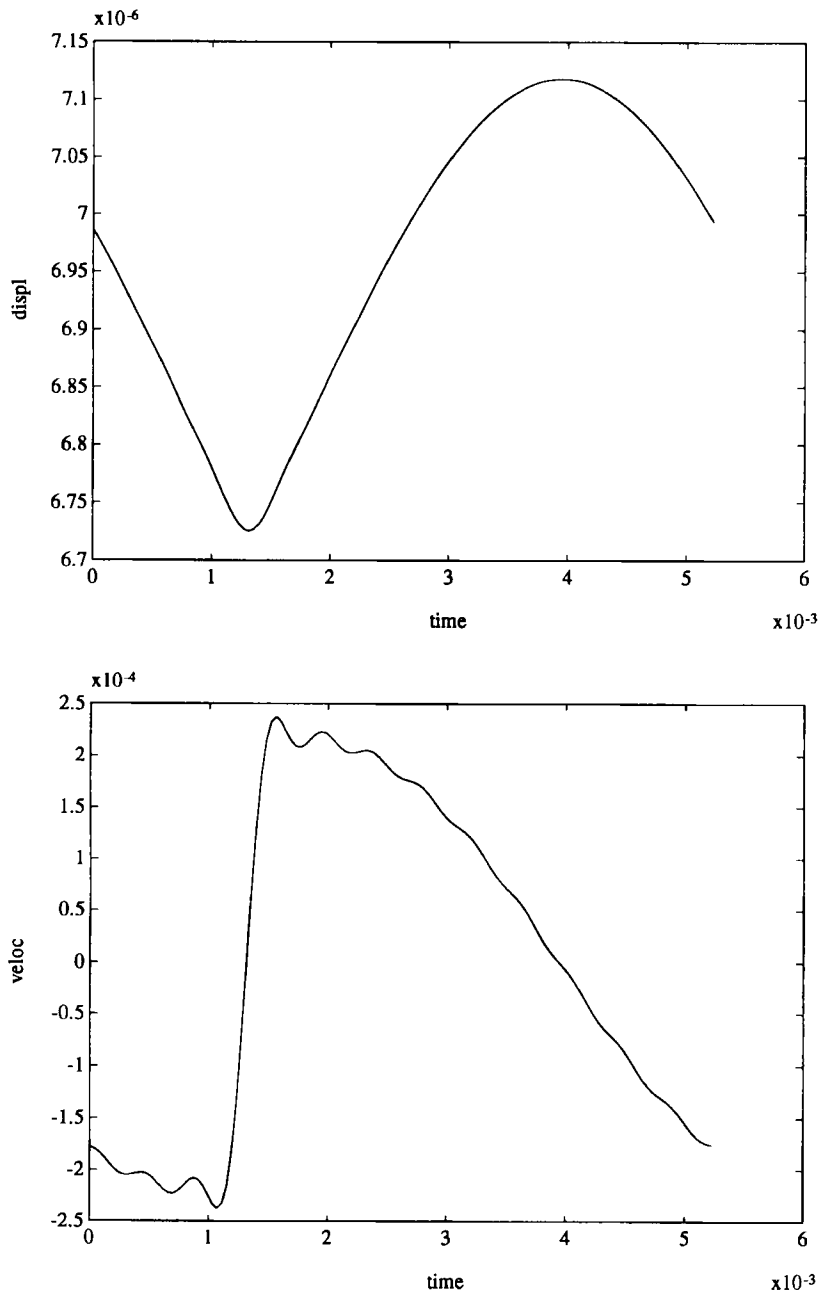


Figure 3. Vertical displacement and velocity of the mass. Excitation frequency: 190 Hz

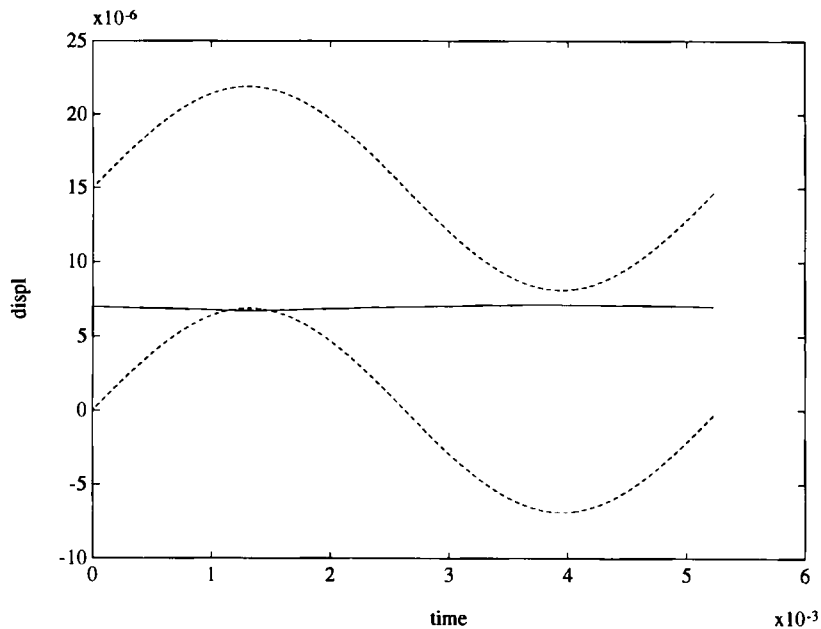


Figure 4. Mass displacement (continuous line) compared to the base and upper-limit displacement (dashed line). Excitation frequency: 190 Hz

5.2. Clamped beam with dry-friction damper

The problem of determining the periodic response of a friction-damped dynamic system has been treated by many authors.^{9, 12, 15} Here we have analysed the response of a clamped beam with a dry-friction damper located at nearly one-fourth of its length, submitted to a periodic excitation on its extreme (see Figure 6). Numerical results are compared to experimental ones for several force levels and for a broad frequency range.

The beam has a total length of $L = 1.28$ m. The friction damper is placed at a distance $L_1 = 0.318$ m from the base. The material properties of the beam are: Young's modulus $E = 2.0 \times 10^{11}$ Pa, Poisson's ratio $\nu = 0.3$ and mass density $\rho = 8125$ kg/m³, its cross-sectional area is $A = 4.64 \times 10^{-4}$ m² and the inertia $I = 1.312 \times 10^{-7}$ m⁴. There are two rigid bodies placed over the beam. The first one is located at the joint with the friction damper: its mass equals $m_1 = 2$ kg and its inertia $J_1 = 0.85 \times 10^{-4}$ kg m². The second body is located at the beam extreme, with mass $m_2 = 0.326$ kg. The dry-friction damper has a spring constant $k = 2.4 \times 10^{-7}$ N/m, the Coulomb friction coefficient equals $\mu = 0.66$ and the compression force at the damper is constant and equal to $N = 372.8$ N.

The beam was modelled by using three finite elements. Structural damping was determined by considering the damper blocked (no sliding was allowed). Rayleigh damping was assumed in the form $\alpha \mathbf{M} + \delta \mathbf{K}$, where $\alpha = 1.03 \times 10^{-4}$ and $\delta = 3.741$. These values correspond to a structural damping $\varepsilon_1 = 2.37$ per cent for the first mode, at frequency 35.2 Hz. The dry-friction law was introduced using a regularized friction force in the form

$$\mathcal{F}_{fr} = -\mu_R(\dot{q})|N| \quad (29)$$

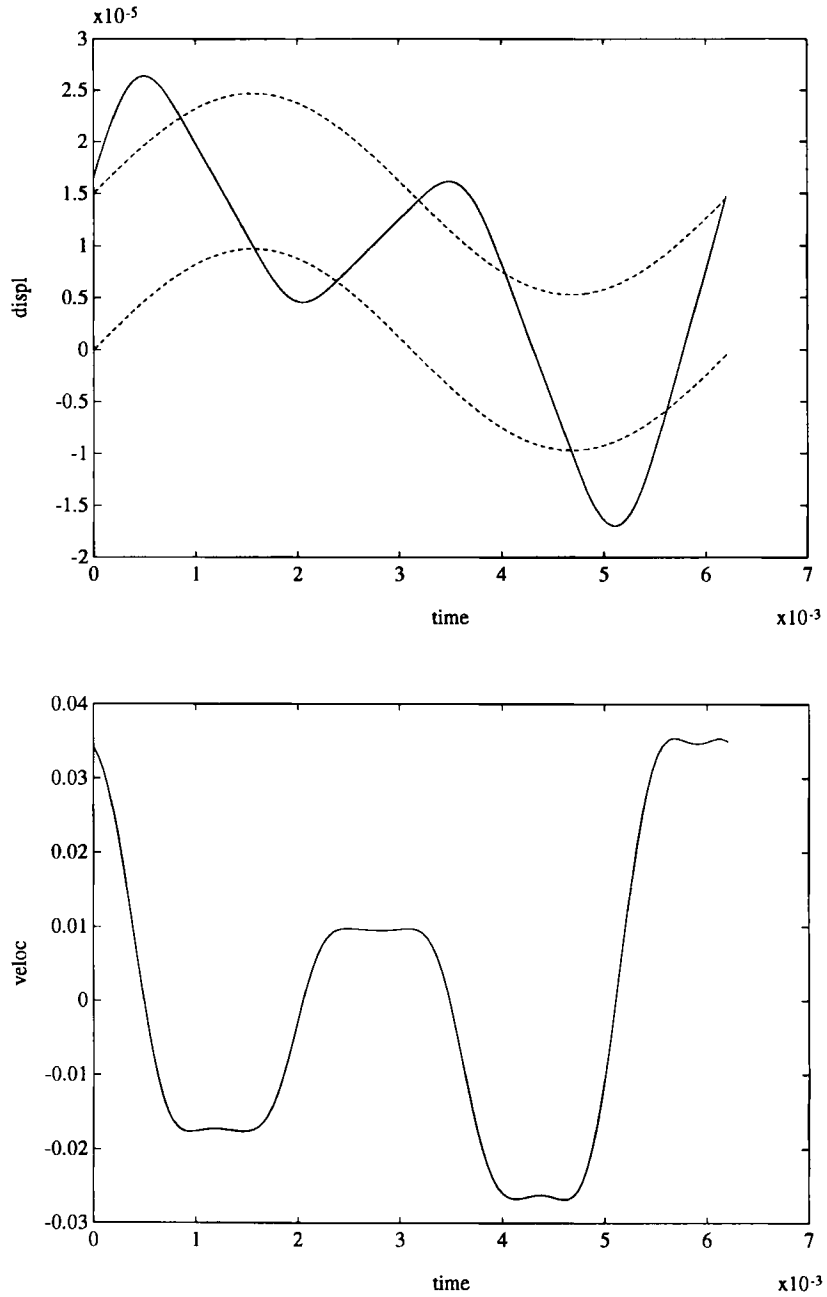


Figure 5. Vertical displacement and velocity of the mass. Excitation frequency: 160 Hz. The base and upper-limit displacements are plotted in dashed lines

where μ_R is a regularized friction coefficient:

$$\mu_R(\dot{q}) = \begin{cases} \mu \dot{q} / \varepsilon_v & \text{if } |\dot{q}| < \varepsilon_v \\ \mu \dot{q} / |\dot{q}| & \text{if } |\dot{q}| \geq \varepsilon_v \end{cases} \quad (30)$$

and N is the normal contact force.

The accuracy of results improves for $\varepsilon_v \rightarrow 0$ (results computed with large values of ε_v are numerically damped). However, the number of iterations necessary for convergence of the non-linear problem increases for small values of ε_v . In order to improve the convergence while keeping accuracy, we have implemented a continuation method in which solutions are iterated by progressively decreasing the value of ε_v up to the point in which two successive solutions do not differ anymore. Once we have got the solution for a given frequency, we predict a solution for the next frequency value in the range of interest using a simple secant scheme and begin a new iterative cycle in which ε_v is varied.¹⁶

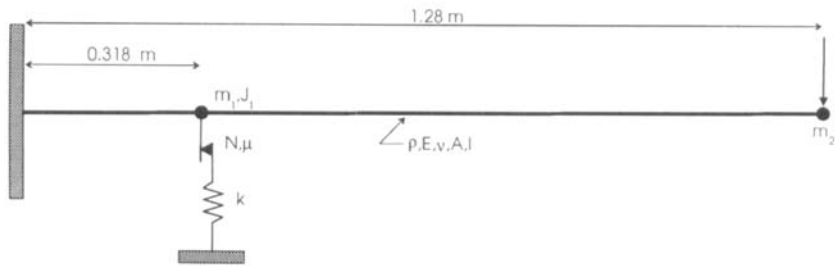


Figure 6. Clamped/free beam with dry-friction damper

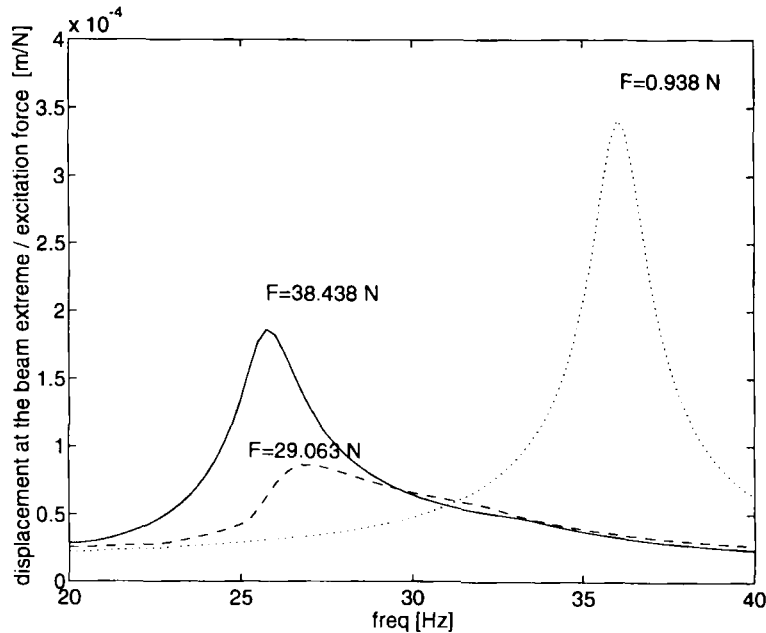


Figure 7. Displacement maximum amplitude at the beam extreme. Numerical results

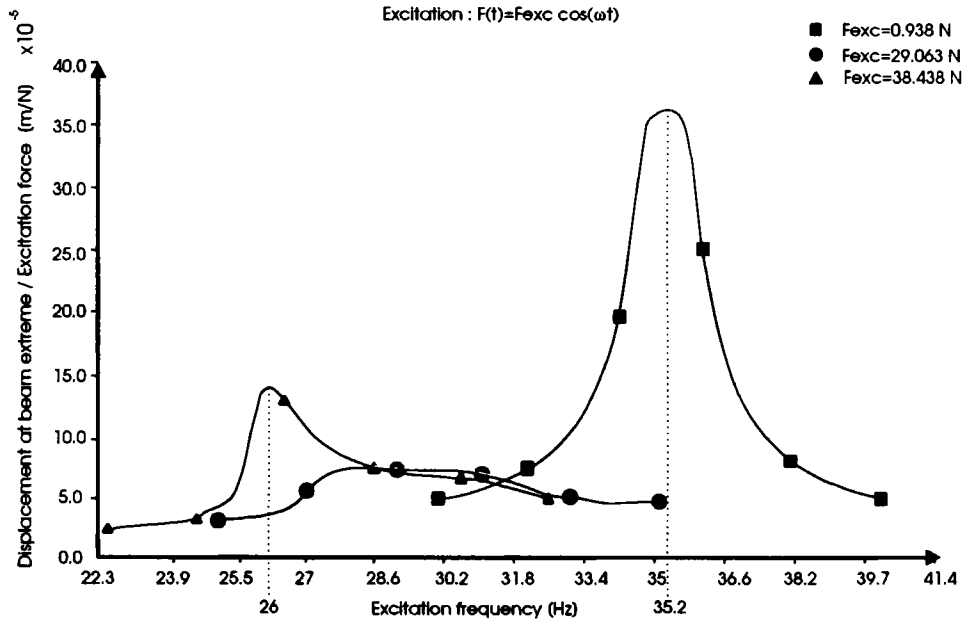


Figure 8. Displacement maximum amplitude at the beam extreme. Experimental results

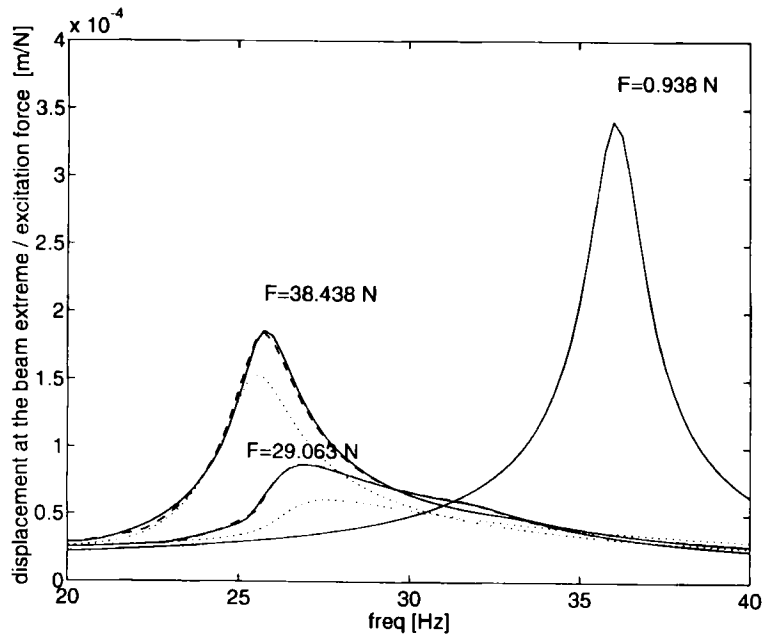


Figure 9. Effect of varying the number of harmonics: (continuous line) 5 harmonics; (dashed line) 3 harmonics; (points) 1 harmonic

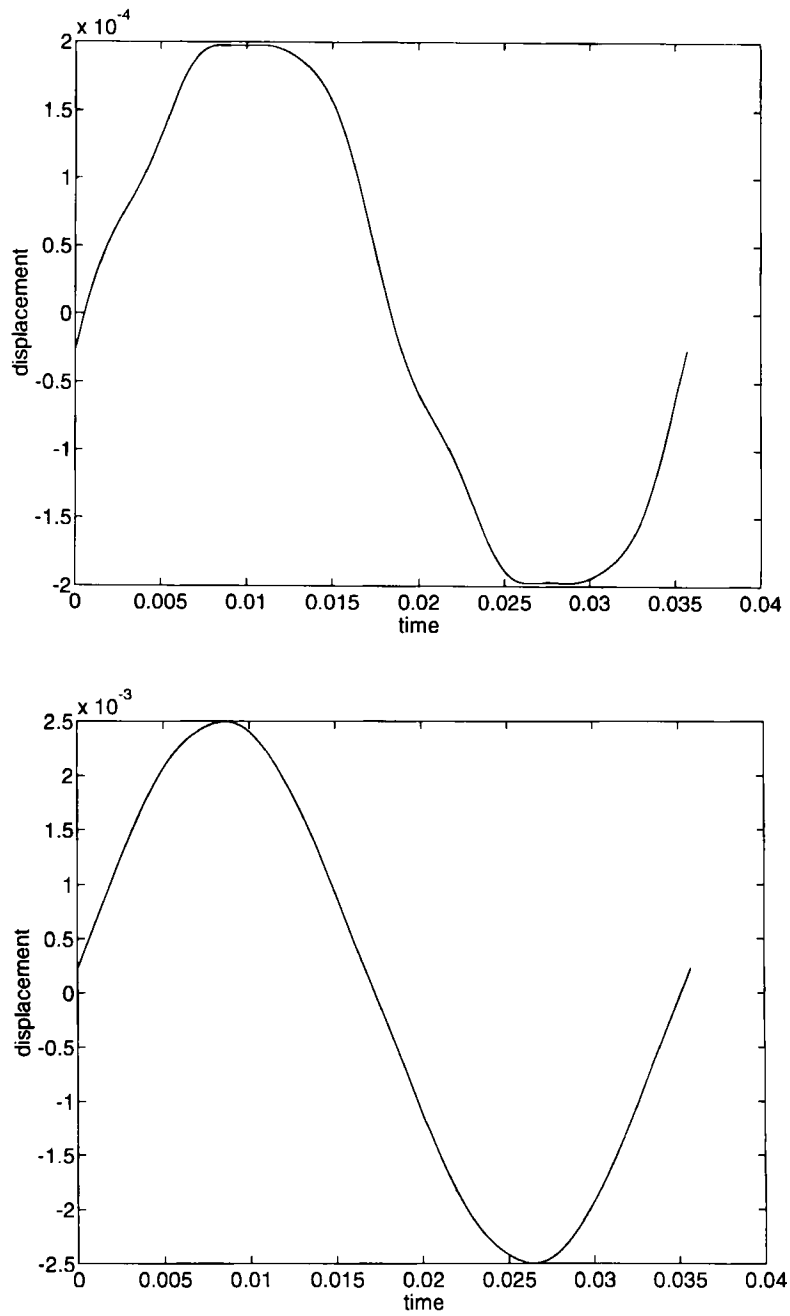


Figure 10. Vertical displacement at nodes 1 and 2. Excitation frequency $f = 28$ Hz

The analysis was made for three different amplitudes ($F_{exc} = 0.938, 29.063$ and 38.438 N). Figure 7 displays the maximum amplitude of displacements measured at the extreme of the beam (divided by the force amplitude) in terms of the frequency of excitation. These results were computed using the five first (odd) harmonics in the Fourier series.

We can see that for small values of excitation, the response is almost linear since the friction damper is blocked. For increasing values of force, the damper unlocks and begins to damp-out some amount of energy from the system. Meanwhile, the frequency of peak is shifted down from 35.2 to 26 Hz.

Figure 8 gives the displacement amplitudes measured from the experimental set-up. We can appreciate that there exists an excellent agreement between peak amplitude frequencies with the numerical computations. Also, the amplitude values and global behaviour for varying frequencies and forces are predicted correctly.

The influence of varying the number of harmonics in the Fourier development is illustrated in Figure 9, in which results computed using one, three and five harmonics are compared. We see that amplitudes corresponding to force levels $F_{exc} = 38.438$ N and $F_{exc} = 29.063$ N are strongly affected when passing from one to three harmonics, while those corresponding to the smallest level of force does not vary. This can be explained by the fact that at the smallest level of force the damper is locked and the system response is linear. Passing from three to five harmonics does not introduce any visible change in the solution, indicating convergence of the process.

The sensitivity of results with respect to the value of the regularizing parameter was also analysed. The computed response was greatly affected by its value. In particular, for $F_{exc} = 0.938$ N, the maximum amplitude was divided by a factor of almost four when passing from $\varepsilon_v = 0.0005$ to $\varepsilon_v = 0.001$ (see Reference 16).

Figure 10 shows the evolution in time of displacements at nodes 1 and 2 when the system is excited at a frequency equal to 28 Hz. We see the stick-slip phenomenon characteristic of Coulomb friction in the evolution of displacements at node 1.

6. CONCLUDING REMARKS

A multiharmonic method to solve non-linear dynamic problems submitted to periodic forcing has been developed. The method is based on a systematic use of the FFT algorithm to project the equations of motion from the time domain to the frequency domain. The resulting non-linear system of equations is exactly linearized, leading to full quadratic convergence rate. Two examples of application have been shown, illustrating the power of the proposed approach.

The method presents enough interest to be implemented in connection with a general software for modelling mechanisms. However, in order to reach this goal, the aspect of handling constraints within the frequency domain approach requires further study. An efficient implementation should also exploit fully the possibility of simplifying the problem based on the presence of localized non-linearities.¹⁴ The model we have used in our second test example to describe the dry-friction force, computed it in terms of the velocity of sliding and of a regularized coefficient of friction. We think it could be better to simulate Coulomb friction phenomena using a displacement model¹⁵ instead. This model requires some modifications in our multiharmonic formulation to get full account of 'history' terms. These subjects will be the objective of further research work.

ACKNOWLEDGEMENTS

The first author acknowledges the EEC, programme ALA/MED, and the FNRS, Belgium, for support during his stay at the University of Liège where this work was performed.

REFERENCES

1. A. Cardona and M. Geradin, 'Time integration of the equations of motion in mechanism analysis', *Comput. Struct.*, **33**, 801–820 (1989).
2. A. Cardona and A. Cassano, 'Integrador temporal de paso variable para análisis dinámico de estructuras y mecanismos', *Revista Internacional de Métodos Numéricos Para Cálculo y Diseño en Ingeniería*, **8**, 439–461 (1992).
3. P. Friedmann, C. E. Hammond and T. H. Woo, 'Efficient numerical treatment of periodic systems with application to stability problems', *Int. j. numer. methods eng.*, **11**, 1117–1136 (1977).
4. P. Friedmann, 'Numerical methods for the treatment of periodic systems with applications to structural dynamics and helicopter rotor dynamics', *Comput. Struct.*, **35**, 329–347 (1990).
5. J. P. Meijaard, 'Direct determination of periodic solutions of the dynamical equations of flexible mechanisms and manipulators', *Int. j. numer. methods eng.*, **32**, 1691–1710 (1991).
6. S. L. Lau and Y. K. Cheung, 'Amplitude incremental variational principle for non-linear vibration of elastic systems', *J. Appl. Mech. ASME*, **48**, 959–964 (1981).
7. S. L. Lau, Y. K. Cheung and S. Y. Wu, 'A variable parameter incrementation method for dynamic instability of linear and nonlinear elastic systems', *J. Appl. Mech. ASME*, **49**, 849–853 (1982).
8. S. L. Lau and W. S. Zhang 'Nonlinear vibrations of piecewise-linear systems by incremental harmonic balance method', *J. Appl. Mech. ASME*, **59**, 153–160 (1992).
9. C. Pierre, A. A. Ferri and E. H. Dowell, 'Multi-harmonic analysis of dry friction damped systems using an incremental harmonic balance method', *J. Appl. Mech. ASME*, **52**, 958–964 (1985).
10. C. Pierre and E. H. Dowell, 'A study of dynamic instability of plates by an extended incremental harmonic balance method', *J. Appl. Mech. ASME*, **52**, 993–997 (1985).
11. F. H. Ling and X. X. Wu, 'Fast Galerkin method and its application to determine periodic solutions of nonlinear oscillators', *Int. J. Nonlinear Mech.*, **22**, 89–98 (1987).
12. T. M. Cameron and J. H. Griffin, 'An alternating frequency/time domain method for calculating the steady-state response of nonlinear dynamic systems', *J. Appl. Mech. ASME*, **56**, 149–154 (1989).
13. Y. B. Kim and S. T. Noah, 'Stability and bifurcation analysis of oscillators with piece-wise linear characteristics—a general approach', *J. Appl. Mech. ASME*, **58**, 545–553 (1991).
14. A. E. Kanarachos and C. N. Spentzas, 'A Galerkin method for the steady state analysis of harmonically excited non-linear systems', *Mech. Machine Theory*, **27**, 661–671 (1992).
15. J. H. Wang and W. K. Chen, 'Investigation of the vibration of a blade with friction damper by HBM', *ASME Paper 92-GT-8*, 1992.
16. T. Coune, A. Cardona and M. Geradin, 'Etude du frottement par méthode multi-harmonique', *LTAS Report VF-88*, University of Liège, Belgium, 1992.